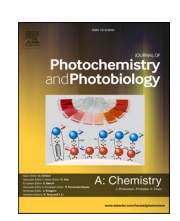
ELSEVIER

Contents lists available at ScienceDirect

#### Journal of Photochemistry & Photobiology, A: Chemistry

journal homepage: www.elsevier.com/locate/jphotochem





## Fluorinated phenyl *meso*-substituents regulating excited state absorption-driven protonation of free-base porphyrins

J.M.S. Lopes <sup>a,b,\*</sup>, A.E.H. Machado <sup>c,d</sup>, A.A. Batista <sup>e</sup>, B.A. Iglesias <sup>f,\*</sup>, P.T. Araujo <sup>g,\*</sup>, N. M. Barbosa Neto <sup>a,\*</sup>

- <sup>a</sup> Institute of Natural Sciences, Graduate Program in Physics, Federal University of Pará, Belém, PA, Brazil
- <sup>b</sup> Department of Physics, Federal University of Roraima, Boa Vista, RR, Brazil
- <sup>c</sup> Graduate Program in Exact and Technological Sciences, Federal University of Catalão, Catalão, GO, Brazil
- <sup>d</sup> Laboratory of Photochemistry and Materials Science, Federal University of Uberlandia, Uberlandia, MG, Brazil
- e Department of Chemistry, Federal University of São Carlos, São Carlos, SP, Brazil
- f Laboratory of Bioinorganic and Porphyrin Materials, Department of Chemistry, CCNE, UFSM, Santa Maria, RS 97105-900, Brazil
- g Department of Physics and Astronomy, University of Alabama, Tuscaloosa, AL, United States

#### ARTICLE INFO

# Keywords: Excited state absorption Photochemistry Porphyrin Photo-protonation Meso-substituents

#### ABSTRACT

Excited state absorption (ESA) has been used as a method to controllably induce photo-protonation of porphyrins in chloroform solution allowing the substitution of continuous UV radiation by visible pulsed light (6 ns pulse width). We explore the role of *meso*-substituents in these photochemical reactions and demonstrate that the number of fluorine atoms linked to the porphyrin's outlying phenyl substituents affects both the protonation formation rate and stability of photo-protonated structures. It is observed that with increasing the number of fluorine atoms the reaction becomes less efficient, and the photo-protonated porphyrins become less stable. Our findings suggest a tuning mechanism to control the ESA-triggered photo-protonation of porphyrins.

#### 1. Introduction

Molecular photochemistry shares frontiers with a great number of areas including materials science [1–3], medicine [4–5], and energy conversion [6–8]. The benefits of using light to promote chemical reactions are mostly associated with selection rules involved in the access of specific excited states of reagents [9–10]. In the one hand, these selection rules are closely dependent on the environmental properties [9–10], including pH, temperature, dielectric constant, and viscosity. On the other hand, photo-induced reactions are strongly regulated by the structure of involved reagents [9–15]. Therefore, even small variations in the composition or geometry of reagents can modulate the yield of photoproduct formation [9–15]. These results show that structure–activity relationships in photochemistry are rather important and require a thorough analysis and understanding.

Porphyrins play important roles as reagents in photochemistry [15–20]. The remarkable photophysical properties of these molecules confer to them characteristic absorption bands spread over the B- (Soret) and Q-bands together with a vast and well-documented number of

excited state deactivation processes including the emission of redfluorescence, hot luminescence, intersystem crossing and excited state charge transfer [21–28]. In addition to these properties, the feasibility of linking groups in the large macrocyclic unit presented by such molecules is seen as a convenient method to tune porphyrin-mediated photochemical reactions.

Recently, the synthetic free-base *meso*-tetra(4-pyridyl)porphyrin (H<sub>2</sub>TPyP) has been employed to promote the excited state absorption (ESA)-driven photochemical reduction of chloroform (CHCl<sub>3</sub>) [29]. The benefits of this approach go beyond the substitution of UV-radiation by visible light and also include the investigation of the role of the reagent's orbital parity in the reaction [16,29]. The overall photochemical reaction resulted in the release of hydrochloric acid (HCl) in the former solution leading to (i) the protonation of the mediator (porphyrin), (ii) exciplex formation, and (iii) possible J-aggregation of protonated porphyrins [29]. Despite the understanding of the rich phenomenology involved in such ESA-driven photochemical reactions, the exploration of both the stability of photoproducts and the role of substituents is still elusive.

E-mail addresses: jefferson.lopes@ufrr.br (J.M.S. Lopes), bernardo.iglesias@ufsm.br (B.A. Iglesias), paulo.t.araujo@ua.edu (P.T. Araujo), barbosaneto@ufpa.br (N.M. Barbosa Neto).

<sup>\*</sup> Corresponding authors.

In this work, a set of fluorine-decorated phenyl free-base porphyrins dissolved in pure chloroform is explored as tunning agents in the aforementioned ESA-driven photochemical reaction. A careful evaluation employing steady-state absorption and fluorescence spectroscopies; time-resolved fluorescence and quantum chemical calculation reveals that ESA-driven photo-protonation of porphyrin, as well as the stability of photoproducts, are ruled by the number of fluorine-atoms linked in the outlying phenyl groups, establishing a reliable mechanism to control the photo-induced process.

#### 2. Materials and methods

#### 2.1. Sample preparation and spectroscopic measurements

The *meso*-tetra(phenyl)porphyrins, both fluorine-free ( $H_2TPP$ ) and fluorinated forms ( $H_2TPF_5P$ ;  $H_2TPF_8P$  and  $H_2TPF_{20}P$ ) were synthesized according to procedures described in the literature [30–33] and their representative structures are depicted in Fig. 1. All porphyrins are dissolved in pure chloroform (CHCl<sub>3</sub>) stabilized with amylene, which was purchased from NEON Inc. and used as received. The concentration of solutions was always set to values below 10  $\mu$ M to avoid the interference of spontaneous aggregate formation and inner filter effects.

Absorption spectra were acquired with a JASCO V-670 spectrophotometer. Steady-state fluorescence spectra were acquired using a setup composed of a Xenon lamp; a monochromator model 300i from ACTON and a portable spectrophotometer from Ocean Optics. The fluorescence signal was detected in a 90° geometry relative to the excitation beam direction. Time-resolved fluorescence experiments were conducted using a Time-Correlated Single Photon Counting (TCSPC) system from Horiba (Delta-Flex model with 27 ps of temporal resolution), equipped with a pulsed laser ( $\lambda_{\rm exc}=352$  nm with 8.0 MHz of repetition rate) as the excitation source. For all samples, the fluorescence decays were collected at the maximum of the steady-state spectra. Emission quantum yields [34–35] were calculated adopting the  $H_2TF_{20}P$  molecule as

Fig. 1. Representative structures of the studied free-base porphyrins. *Meso*-tetra(phenyl)porphyrin ( $H_2TPP$ ); *meso*-5-(pentafluorophenyl)-10,15,20-tri (phenyl)porphyrin ( $H_2TPF_5P$ ); *meso*-tetra(2,5-fluorophenyl)porphyrin ( $H_2TPF_8P$ ) and *meso*-tetra(pentafluorophenyl)porphyrin ( $H_2TPF_2OP$ ).

standard [28] and applying Eq. (1), where,  $\Phi_{sa}$  and  $\Phi_{st}$  account for the quantum yields of the sample (sa) and standard (st) solution, respectively. The quantities  $Abs_{st}$  ( $F_{st}$ ) and  $Abs_{sa}$  ( $F_{sa}$ ) are the absorbances at 420 nm (the integrated fluorescence intensities) for the sample and standard solutions. Both sample and standard were dissolved in chloroform.

$$\Phi_{sa} = \Phi_{st} \frac{Abs_{st}}{Abs_{so}} \frac{F_{sa}}{F_{st}} \tag{1}$$

Considering the excited state lifetimes  $(\tau)$  and  $\Phi_{sa}$ , both the radiative  $(k_r)$  and nonradiative  $(k_{nr})$  relaxation rates of the first singlet excited state can be obtained using Eqs. (2) and (3) [34–35].

$$k_{r} = \frac{\Phi_{sa}}{\tau} \tag{2}$$

$$k_{nr} = \frac{1}{\tau} [1 - \Phi_{sa}] \tag{3}$$

#### 2.2. Excited state absorption-driven photochemistry

A frequency-doubled Q-switched Nd-YAG laser, from Quantel (Q-smart 100 model, 6.0 ns FWHM, 532 nm excitation, 20 Hz of repetition rate) was used as the pulsed-radiation source. Each pulse presents a nominal fluence of  ${\sim}836$  mJ/cm². Samples were submitted to the total fluence of  ${\sim}300$  J/cm² in intervals of  ${\sim}50$  J/cm². Quantitative analysis of pulsed irradiation was performed by considering the effectively absorbed fluence (absorbed photon density) instead of incident fluence. In brief, by conservation, the relation between the incident (F<sub>I</sub>), transmitted (F<sub>T</sub>) and absorbed (F<sub>A</sub>) fluences is written as F<sub>I</sub> = F<sub>T</sub> + F<sub>A</sub>. Normalizing it by F<sub>I</sub> we have [34]  $1-\frac{F_T}{F_I}=\frac{F_A}{F_I}$ . From Lambert-Beer law,  $\frac{F_T}{F_I}=10^{-A(\lambda)}$  (with  $A(\lambda)$  corresponding to absorbance at the incident wavelength, for the non-irradiated solution) resulting in Eq. (4).

$$F_{A} = F_{I} (1 - 10^{-A(\lambda)}) \tag{4}$$

Inspecting the characteristic maximum absorption values at the B-band assigned to the non-protonated (A) and protonated (A<sub>P</sub>) porphyrins we obtained absorbance ratios  $R_F = \frac{A_P}{A}$ , which evolutions were plotted as a function of  $F_A$  allowing the calculation of parameters related to the photochemical reaction. Therefore, each sample has yielded characteristic curves, that could be fitted by applying an exponential function defined in Eq. (5).

$$R_{F} = Be^{[kF_{A}]} \tag{5}$$

The parameters B; and k stand for the exponential amplitude, and photo-protonation rate (given in cm<sup>2</sup>/J) respectively.

#### 2.3. Quantum chemical calculations

The molecular structures were optimized employing the *meta*-GGA M06 DFT hybrid functional [36], while the electronic spectra were calculated using the time-dependent version of DFT, applying the CAM-B3LYP hybrid functional [37] in combination with the DGDZVP double-zeta atomic basis set [38]. The electronic spectra were obtained using the same atomic basis set, in calculations performed considering the 60 first singlet excited states. All calculations were performed in the solvation environment simulated using the integrated equation formalism polarizable continuum model (IEFPCM) [39–40], considering chloroform as the solvent. All calculations were done using the software Gaussian 09, rev. E.01 [41]. Orbitals and electron densities over the macrocycles were obtained using the software GaussView 5.

#### 3. Results and discussions

#### 3.1. Insights from the photophysical processes

Due to the sensitivity of the porphyrin's excited state to structural modifications [22-23], we initially explore the role played by fluorine atoms on the absorption and emission properties of H2TPP solution. Fig. 2a and b show that the presence of fluorine atoms at outlying positions progressively causes blue shifts of the most intense B- and Qabsorption bands of fluorinated porphyrins regarding H2TPP. Considering the Gouterman four orbitals model [21-23], these shifts can be associated with an overall modification in the conjugation length of the  $\pi$  structure of the macrocycle, which can be understood as a fluorinedependent variation in the energy gap of involved transitions. Taking into account the fact that electronegative atoms like fluorine can pull electrons from conjugated structures such as phenyl and the macrocycle itself [24,42-43], it is possible to infer that the macrocycle is also probably disturbed by the electron withdrawing character achieved in the substituents. Therefore, the higher the number of appended fluorine atoms, the greater (lower) the energy gap (the electronic density) at the macrocycle ring, which directly impacts the porphyrins' spectroscopic signatures [21,25,28]. Taking H<sub>2</sub>TPP as the reference, a careful inspection of the B-band in the absorption spectrum reveals relative shifts of 7.11 meV (H2TPF5P), 28.66 meV (H2TPF8P), and 35.91 meV  $(H_2TPF_{20}P)$ , respectively. For the  $Q_v(0,1)$ -band, these relative shifts are greater than the shifts of the B-band, displaying the values of 14.05 meV, 37.84 meV, and 47.49 meV for H<sub>2</sub>TPF<sub>5</sub>P, H<sub>2</sub>TPF<sub>8</sub>P, and H<sub>2</sub>TPF<sub>20</sub>P, respectively. This behavior indicates that fluorine atoms affect distinctly the first and the second excited states of porphyrins since B-bands (O-bands) arise from  $S_0 \rightarrow S_2$  ( $S_0 \rightarrow S_1$ ) transitions in the macrocycle ring [21-23]. The reason for such behavior is the influence of the fluorine atoms on the conjugation length of the macrocycle, which is possibly caused by the distortion of the carbon atoms'  $\pi$ -orbitals in the porphyrin ring. Furthermore, the calculations show that the electronic densities at the macrocycle are affected by the presence of outlying fluorine atoms, see Fig. S1 from Supplementary Material (SM). It is also verified that electronic density is less localized at the center of the macrocycle for the  $H_2TPF_{20}P$  molecule in comparison to the  $H_2TPP$ .

Together with the occurrence of the overall blue shift in the absorption spectra, there is a strong dependence between the presence of fluorinated substituents and the vibronic structure of the Q-band. Sig-

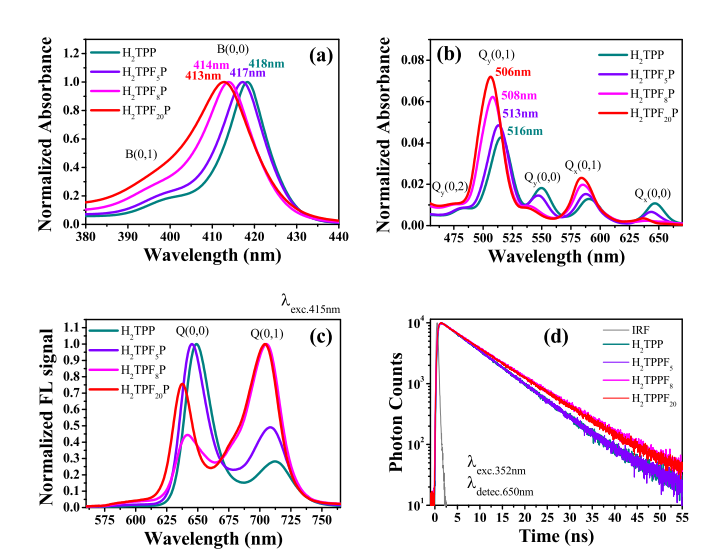


Fig. 2. Normalized absorption spectra at (a) B-band and (b) Q-band; (c) Fluorescence (FL) spectrum ( $\lambda_{\rm exc} = 415$  nm) and (d) fluorescence decays ( $\lambda_{\rm detec.} = 650$  nm) of fluorinated phenyl porphyrins (H<sub>2</sub>TPP (dark cyan), H<sub>2</sub>TPF<sub>5</sub>P (violet), H<sub>2</sub>TPF<sub>8</sub>P (magenta) and H<sub>2</sub>TPF<sub>20</sub>P (red) dissolved in CHCl<sub>3</sub>.

nificant variations in the relative intensity of peaks associated with the vibronic progressions at B- and Q-bands indicate that fluorine atoms affect the relative displacement between potential energy surfaces involved in the transitions (ground, first, and second excited states) which is in agreement with the literature [25,28].

Turning attention to the steady-state emission spectra, it is verified by following the absorption features that fluorine atoms also cause blue shifts in the spectra and drive modifications on the  $H_2TPP$  porphyrin's vibronic features, see Fig. 2c. In  $H_2TPF_8P$  and  $H_2TPF_{20}P$ , the vibronic Q(0,1) emission band becomes more intense than its Q(0,0) counterpart, reinforcing the role of substituents on the vibronic progressions observed for the absorbance at the Q-band. Excited state deactivation kinetics are also affected by the number of fluorine atoms. As verified in Fig. 2d and Table 1, although excited state lifetimes are only slightly modified, both the emission quantum yields  $\Phi_{\text{sa}}$  and deactivation rates  $(k_{\text{r}}$  and  $k_{\text{nr}})$  decrease as a function of the number of linked fluorine atoms.

Note that, while  $\tau$  and  $k_{nr}$  are barely affected,  $k_r$  undergoes significant modifications. The decrease of 48 % in the former  $H_2TPP$  radiative quantum yield observed in  $H_2TPF_{20}P$  can be mostly attributed to a reduction in the porphyrin's  $k_r$ , see Table 1. From Fermi's golden rule, the deactivation rates are associated with the downward transition's dipole strength which, in turn, depends on the dipole transition moment and consequently on the electronic density of involved states [34–35,44–45]. This trend reinforces the fact that fluorine atoms are affecting the electron population of involved  $\pi$  and  $\pi^*$  orbitals in the transitions.

### 3.2. The impact of fluorinated phenyl substituents on the photo-protonation

Irradiation of the samples with a pulsed 532 nm laser source was necessary to induce excited state absorption-driven photo-protonation as reported elsewhere [29,46]. Fig. 3 shows that the former spectroscopic signatures smoothly evolve when the samples are irradiated by the pulsed laser, resulting in the formation of novel red-shifted peaks which can be promptly assigned to corresponding protonated porphyrins [16,18,43,47-51]. To support the occurrence of the ESA-driven photochemical reaction, all samples were also excited with a continuous laser source ( $\lambda_{exc} = 532$  nm) which has not implied any modification in the spectrum, confirming that ESA plays a fundamental role in the formation of photoproducts. Moreover, according to the literature, fluorinated porphyrins are good ESA absorbers when submitted to similar conditions regarding that adopted herein [18,43,48,50,52]. Similar to what occurs for H2TPyP [29], the ESA-triggered photo-protonation of fluorinated phenyl porphyrins in chloroform is assumed to follow the well-known dye-mediated photo-oxi-reduction of solvent [16,29,53-56]. In brief, the excited porphyrins donate electrons from their macrocycle ring toward CHCl3, finally resulting in the formation of hydrochloric acid (HCl) and other unstable products [16].

As shown in Fig. 3, the photo-protonation process is mainly ruled by the number of fluorine atoms appended in the substituents. The absorbance and, consequently, the concentration of protonated species, is

Table 1 Fluorescence parameters for the fluorinated phenyl porphyrins, where  $\tau=$  fluorescence decay lifetime,  $\Phi_{sa}=$  fluorescence quantum yield,  $k_r=$  radiative decay rate, and  $k_{nr}=$  non-radiative decay rate. All molecules are dissolved in CHCl $_3$  and the radiative quantum yield of  $H_2TPF_{20}P$  in chloroform ( $\Phi_{st}=1.79\times 10^{-2})$  was taken as standard [28].

Porphyrin	$\tau~\times 10^{-9}~s$	$\Phi_{sa} \ \times 10^{-2}$	$k_r \; {\times} 10^6 \; S^{-1}$	$k_{nr} \times 10^6 \; S^{-1}$
H <sub>2</sub> TPP	8.00 (±0.02)	3.4 (±0.1)	4.3 (±0.1)	120.6 (±0.1)
$H_2TPF_5P$	$8.00~(\pm 0.02)$	$2.7~(\pm 0.1)$	$3.3~(\pm 0.1)$	$121.6~(\pm 0.1)$
$H_2TPF_8P$	$9.10~(\pm 0.02)$	$2.0~(\pm 0.1)$	$2.2~(\pm 0.1)$	107.7 ( $\pm 0.1$ )
$H_2TPF_{20}P$	$9.00~(\pm 0.02)$	$1.8~(\pm 0.1)$	$2.0~(\pm 0.1)$	107.6 ( $\pm 0.1$ )

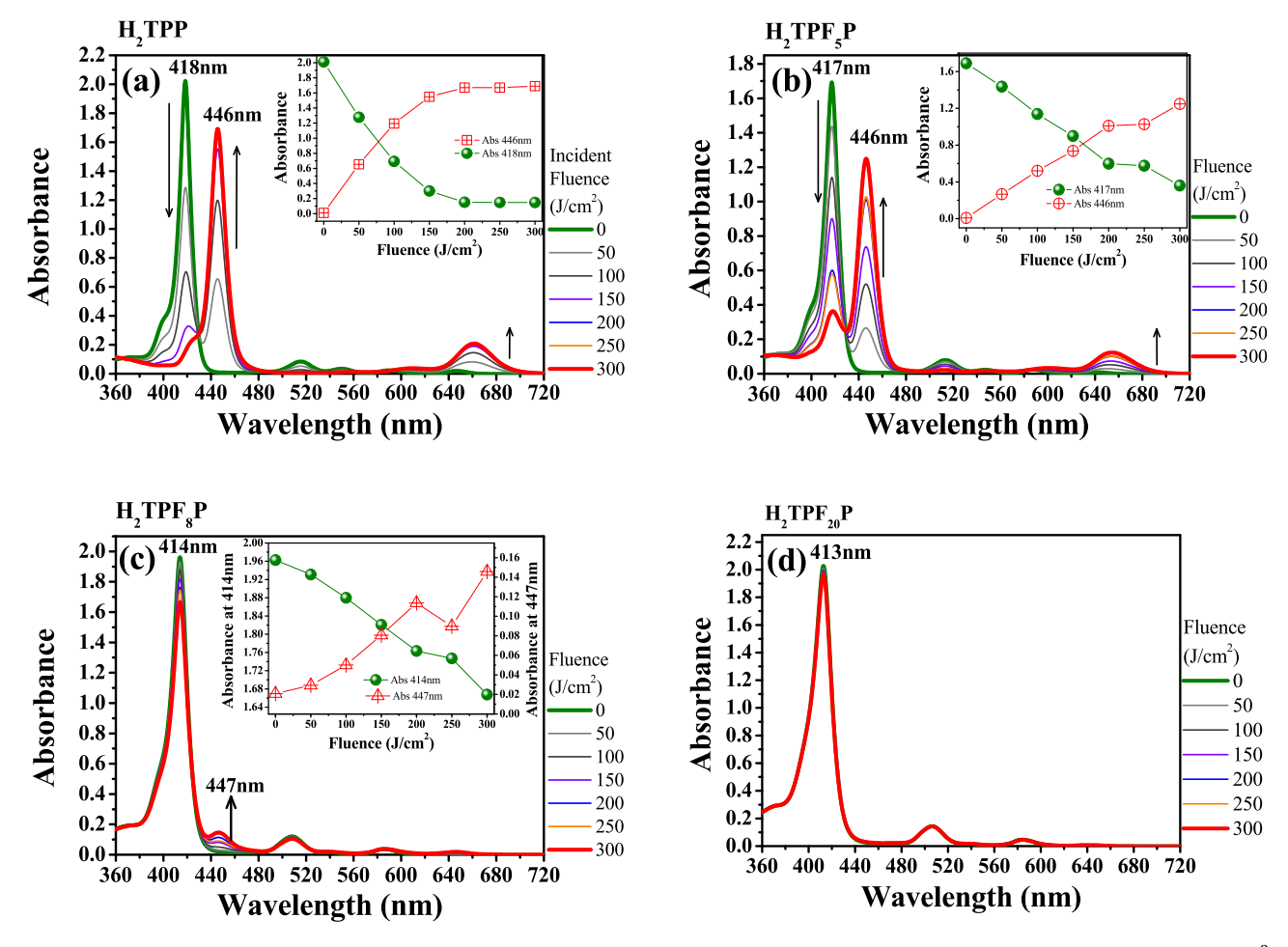


Fig. 3. Absorption spectra evolution for (a)  $H_2TPP_5$ ; (b)  $H_2TPP_5P$ ; (c)  $H_2TPP_5P$  and (d)  $H_2TPP_2P$  porphyrins as a function of incident fluence (0–300 J/cm<sup>2</sup>). The insets in these figures show the incident fluence-dependent evolution of the most intense B-band, associated with pristine, and the band located around 446 nm, assigned to protonated species.

maximum for  $H_2TPP$  and almost negligible for  $H_2TPF_{20}P$ . Differently from  $H_2TPyP$ , the main B-band of the remnant pristine porphyrins (unconverted reagent) investigated herein does not undergo any shift [29] during the process, implying that outlying substituents are not being protonated [29,51]. The absence of protonation at the outlying substituent sites can be understood in terms of affinity and stability between protons and the electronegative atoms in the porphyrin periphery. In the case of pyridyl substituted porphyrins, there's a well-known  $H^+$ -N favorable interaction mechanism [51], involving the donation of a proton from HCl and its reception at the nitrogen atoms from the pyridyl. Although  $H^+$ -F interaction could lead to a similar process, this interaction is reported weak and unstable [57–59].

Supporting the assignment of photo-protonation, the fluence-dependent evolution of steady-state fluorescence spectra and excited state decay kinetics of  $H_2TPP$ ,  $H_2TPF_5P$ , and  $H_2TPF_8P$  porphyrins are shown in Fig. S2 from SM. It is observed that in agreement with absorption spectra, emission signals of  $H_2TPF_5P$  and  $H_2TPF_8P$ , originally containing features solely related to the unprotonated species, become multi-structured at  $300~\text{J/cm}^2$  comprising a superposition of fluorescence peaks and decays of remnant unprotonated and the newly formed protonated species. For the case of  $H_2TPP$ , the initial features are fully converted at  $300~\text{J/cm}^2$ , in agreement with absorption spectra. The  $H_2TPF_{20}P$  molecule had its emission features unaltered through irradiation agreeing with its absorption spectrum.

To quantify the process, the ratio between absorbances probed at the most intense peaks of the B-bands of protonated  $(A_P)$  and pristine (A) porphyrins are inspected as a function of  $F_A$ . Herein, the use of  $F_A$ 

instead of  $F_I$  assures a homogeneous correction of the response of each sample to the incident excitation wavelength (532 nm). In Fig. 4 it can be observed that each evaluated porphyrin follows its proper behavior, endorsing the role played by substituents. Each curve was fitted by applying Eq. (5) demonstrating that photo-protonation of  $H_2TPP$  is the most efficient among all samples. In fact,  $H_2TPP$  ESA-triggered core protonation is almost twice as efficient as the previously reported  $H_2TPyP$  ESA-triggered core protonation under the same conditions (Fig. S3 from SM) and approximately-seven times more efficient than  $H_2TPF_8P$  ESA-triggered core-protonation. Fig. 4b shows, higher to lower, the photo-protonation rates for:  $H_2TPP$  (~290.64 × 10<sup>-3</sup> cm²/J) >  $H_2TPF_5P$  (~208.06 × 10<sup>-3</sup> cm²/J) >  $H_2TPF_8P$  (~43.58 × 10<sup>-3</sup> cm²/J) >  $H_2TPF_9P$  (~0.00 cm²/J).

A possible explanation for the observed rates is that fluorine atoms could be affecting the overall porphyrin-mediated photo-oxi-reduction of chloroform. In this hypothesis, electron withdrawing effect could prevent electron transfer from the porphyrin toward chloroform which would significantly reduce the amount of HCl photochemically formed and, consequently, lead to a decrease in the photo-protonation rate. This would imply that in the case of  $H_2TPF_{20}P$  no significant amount of HCl is released in the solution explaining its almost null photo-protonation rate. To test this hypothesis, we irradiated  $H_2TPF_{20}P$  under the same concentration, solvent, and fluence conditions, adopted early, and after this processing, an analog porphyrin, the thienyl substituted free-base porphyrin ( $H_2TThP$  dissolved in chloroform with the concentration of  $2.0 \,\mu\text{M}$ ) was added to the solution to act as an acid sensor. This molecule displays characteristic B- and Q- absorption bands [28] located at longer

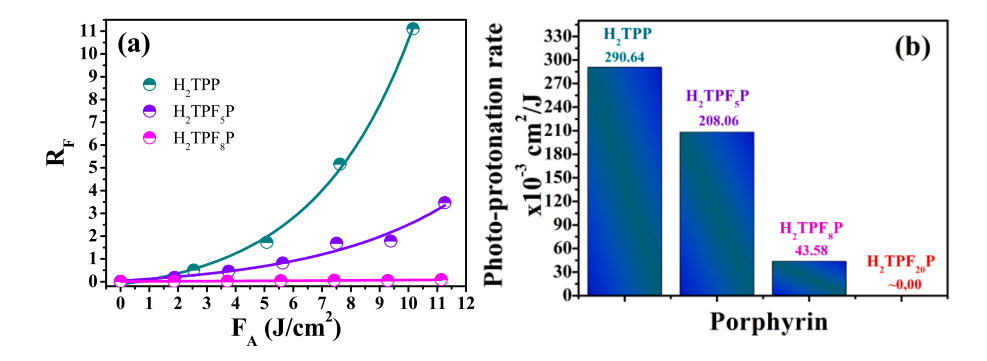


Fig. 4. (a) Evolution of absorbance ratios  $(R_F = \frac{A_P}{A})$  as a function of  $F_A$  for  $H_2$ TPP (dark cyan semi-filled circles),  $H_2$ TPF $_5$ P (violet semi-filled circles), and  $H_2$ TPF $_8$ P (magenta semi-filled circles) porphyrins. In (a) the continuous lines represent the corresponding fitting of  $R_F$ . (b) Photo-protonation rates obtained employing Eq. (5).

wavelengths in comparison to the fluorinated species and is extremely sensitive to acids due to its easy protonation [29]. In this case, the acid sensor and irradiated  $H_2TPF_{20}P$  were mixed in a 1:200 (v/v) proportion. The results demonstrate that HCl is being formed in the solution, i.e., the acid probe ( $H_2TThP$ ) undergoes protonation and forms a novel and redshifted B-band, see Fig. S4 from SM. This scenario, however, does not support the occurrence of a null photo-protonation rate for  $H_2TPF_{20}P$  because of a possible fluorine-drive turn-off of chloroform decomposition.

A close relationship between the stability of photo-protonated porphyrins and the decorated substituents was also verified. After being irradiated, the samples were stored in sealed cuvettes under dark and temperature-controlled conditions (room temperature  $\sim\!22.5\,^\circ\text{C}$ ) for 24 h. The absorption spectrum of each sample was inspected after this period without opening the sealed cuvette resulting in Fig. 5, where it is demonstrated that the capability to hold the protons at the center of the macrocycle is closely dependent on the number of fluorine atoms appended in the phenyl group.

After 24 h of sample storage, the protonated  $H_2TPP$  counterpart  $(H_4TPP^{2+})$  is found to be stable, and no evidence of photoproduct degradation (dissociation) is observed. Oppositely, for both the protonated forms of  $H_2TPF_5P$  and  $H_2TPF_8P$ , it is observed that in the first (second) case a partial (full) reversion of photoproducts occurs, see Fig. 5b and c. Indeed, the higher the number of fluorine atoms linked, the more unstable the protonated species. Similar to what has been observed for the photo-protonation rates, the stability of phenyl porphyrins follows the order (from most to less stable):  $H_2TPP > H_2TPF_5P > H_2TPF_8P$ . This behavior suggests that the presence of outlying fluorine atoms difficult the insertion and permanence of the extra hydrogen atoms at the center of the porphyrin ring. Such a fact could be explained

by the role of electron withdrawal in the porphyrin structures. From a mechanistic point of view, besides affecting the overall electronic density of the macrocycle (as shown in Fig. S1 from SM), electron withdrawal could pull electrons from the macrocycle center and enhance the positive character of the nitrogen sites, which could drastically affect the photo-protonation process [24,42]. In this case, the Mulliken charges at these nitrogen sites were expected to vary accordingly with the number of appended fluorine atoms. However, quantum chemical calculation demonstrates that this parameter is not significantly affected by substituents: 0.461 (H<sub>2</sub>TPP<sub>2</sub>), 0.460 (H<sub>2</sub>TPF<sub>5</sub>P), 0.463 (H<sub>2</sub>TPF<sub>8</sub>P), and 0.464 (H<sub>2</sub>TPF<sub>2</sub>0P), see Fig. S5 from SM. This result rules out the occurrence of a possible increase in the positive character of the nitrogen positions due to substituents.

An additional explanation for the observed results could be associated with the formation of steric barriers due to appended fluorine, which would be affecting the capacity of protons to reach the center of the macrocycle. In other words, despite being porphyrins still capable to decompose  $CHCl_3$  and form HCl, there is stiff competition between the insertion of protons at the central portion of the macrocycle (nitrogen atoms) or in the fluorine atoms of substituents. As already discussed, the  $H^+$ -F bonding is considered weak [57–59] and according to Fang et al. [51], protonation of *meso*-substituents would result in a small but still observable red-shift in the most intense B-band of pristine porphyrin [29], which does not occur herein, see Fig. 3. Therefore, it is unlikely that protons are being captured by the outlying substituents prior to the macrocycle's core.

#### 4. Conclusion

A set of fluorinated phenyl porphyrins was explored to address the

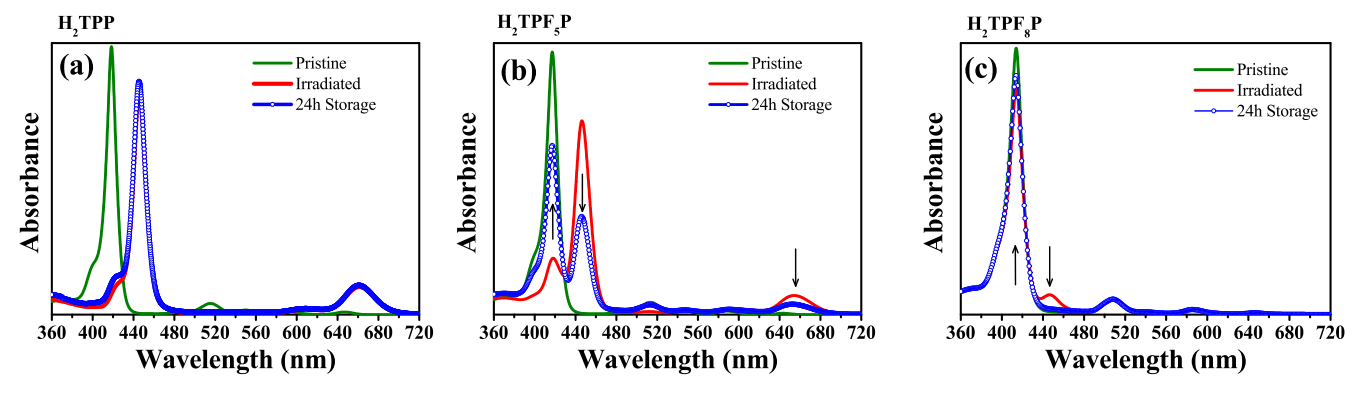


Fig. 5. Evaluation of the stability of photo-protonated (a)  $H_2TPP$ ; (b)  $H_2TPF_5P$ ; and (c)  $H_2TPF_8P$  porphyrins, storage at room temperature and dark conditions for 24 h.

elusive structure—activity relationships in the porphyrin-assisted ESA-driven photodecomposition of chloroform. Since this reaction leads to the photo-protonation of the porphyrins, the characteristic spectroscopic signatures could be used to obtain the reaction rate and to track the stability of protonated porphyrins. It was demonstrated that the number of fluorine atoms appended in the substituents plays a significant role in both features. We observed that the fluorine-free *meso*-tetra phenyl porphyrin is a good candidate for applications involving ESA-triggered photo-protonation because the formation of the protonated counterpart is more efficient, and the specie is more stable when compared to other evaluated porphyrins. This work also brings a tuning mechanism for ESA-driven photo-protonation of porphyrins through the adoption of electronegative ligands in the *meso* groups.

#### CRediT authorship contribution statement

J.M.S. lopes: Conceptualization, Data curation, Writing – original draft, Writing - review & editing, Visualization, Investigation, Validation, Formal analysis, Methodology. A.E.H. Machado: Funding acquisition, Data curation, Writing - review & editing, Visualization, Investigation, Validation, Formal analysis, Methodology, Resources, Software, A.A. Batista: Funding acquisition, Writing – review & editing, Visualization, Validation, Methodology; Resources; Project administration. B.A. Iglesias: Funding acquisition, Data curation, Writing - original draft, Writing - review & editing, Visualization, Validation, Methodology, Resources. P.T. Araujo: Conceptualization, Funding acquisition, Data curation, Writing - original draft, Visualization, Investigation, Validation, Formal analysis, Methodology, Supervision, Resources, Project administration. N.M. Barbosa Neto: Conceptualization, Funding acquisition, Data curation, Writing - original draft, Writing - review & editing, Visualization, Investigation, Validation, Formal analysis, Methodology, Supervision, Resources, Project administration.

#### **Declaration of Competing Interest**

The authors declare that they have no known competing financial interests or personal relationships that could have appeared to influence the work reported in this paper.

#### Data availability

Data will be made available on request.

#### Acknowledgments

The authors are indebted to Brazilian agencies: CNPq under Grants No. [306147/2020-3], FAPESPA and CAPES under Grant No. [Finance Code 001; AUXPE 88881.159129/2017-01], FAPEMIG, National Institute for Science and Technology on Organic Electronic (INEO), and National Science Foundation (NSF) under Grant No. [1848418] for the financial support. NMBN is especially grateful to Fulbright Foundation for the Visiting Professor Scholarship Award. B. A. Iglesias also to thanks CNPq grants (409.150/2018-5 and 304.711/2018-7), and the Research Support Foundation of the State of Rio Grande do Sul – FAPERGS (21/2551-0002114-4) for the financial support. The authors are grateful to professor Sanclayton Moreira, from the Graduate Program in Physics of the Federal University of Para for granting access to his experimental facilities.

#### Appendix A. Supplementary data

Supplementary data to this article can be found online at https://doi.org/10.1016/j.jphotochem.2023.114568.

#### References

- [1] N.M.B. Neto, M.D.R. Silva, P.T. Araujo, R.N. Sampaio, Photoinduced self-assembled nanostructures and permanent polaron formation in regioregular poly (3-hexylthiophene), Adv. Mater. 30 (2018) 1705052.
- [2] S. Juodkazis, V. Mizeikis, K.K. Seet, M. Miwa, H. Misawa, Two-photon lithography of nanorods in SU-8 photoresist, Nanotechnology 16 (2005) 846–849.
- [3] H.B. Sun, S. Kawata, Two-photon photopolymerization and 3D lithographic microfabrication, Adv. Polym. Sci. 170 (2004) 169–273.
- [4] A.E. O'Connor, W.M. Gallagher, A.T. Byrne, Porphyrin and nonporphyrin photosensitizers in oncology: preclinical and clinical advances in photodynamic therapy, Photochem. Photobiol. 85 (2009) 1053–1074.
- [5] M. Khurana, H.A. Collins, A. Karotki, H.L. Anderson, D.T. Cramb, B.C. Wilson, Quantitative in vitro demonstration of two-photon photodynamic therapy using Photofrin® and Visudyne®, Photochem. Photobiol. 83 (2007) 1441–1448.
- [6] K. Kalyanasundaram, Photophysics, photochemistry and solar energy conversion with tris(bipyridyl)ruthenium(II) and its analogues, Coord. Chem. Rev. 46 (1982) 159–244.
- [7] C.G. Garcia, J.F. De Lima, N.Y. Murakami Iha, Energy conversion: From the ligand field photochemistry to solar cells, Coord. Chem. Rev. 196 (2000) 219–247.
- [8] L. Andreoni, M. Baroncini, J. Groppi, S. Silvi, C. Taticchi, A. Credi, Photochemical energy conversion with artificial molecular machines, Energy Fuels 35 (2021) 18900–18914
- [9] N. Turro, Modern Molecular Photochemistry, University Science Books, Mill Valley, 1991.
- [10] N.J. Turro, Molecular photochemistry, Chem. Eng. News 45 (1967) 84–95.
- [11] Ł.W. Ciszewski, K. Rybicka-Jasińska, D. Gryko, Recent developments in photochemical reactions of diazo compounds, Org. Biomol. Chem. 17 (2019) 432–448.
- [12] G. Siano, S. Crespi, S.M. Bonesi, Substituent and surfactant effects on the photochemical reaction of some aryl benzoates in Micellar green environment, Photochem. Photobiol. 97 (2021) 1298–1309.
- [13] T. Nyokong, Effects of substituents on the photochemical and photophysical properties of main group metal phthalocyanines, Coord. Chem. Rev. 251 (2007) 1707–1722.
- [14] A. Manfrin, A. Hänggli, J. Van Den Wildenberg, K. McNeill, Substituent effects on the direct photolysis of benzotrifluoride derivatives, Environ. Sci. Technol. 54 (2020) 11109–11117.
- [15] J.M.S. Lopes, S.N. Costa, E. Silveira-Alves Jr, A.A. Batista, P.J. Gonçalves, L. R. Dinelli, P.T. Araujo, N.M. Barbosa Neto, Singlet oxygen generation and spectroscopic properties of supramolecular zinc meso tetra (4-pyridyl) porphyrin bearing outlying ruthenium groups, Braz. J. Phys. (2022) 38–40.
- [16] Z. Muñoz, A.S. Cohen, L.M. Nguyen, T.A. McIntosh, P.E. Hoggard, Photocatalysis by tetraphenylporphyrin of the decomposition of chloroform, Photochem. Photobiol. Sci. 7 (2008) 337–343.
- [17] T. Higashino, H. Imahori, Porphyrins as excellent dyes for dye-sensitized solar cells: Recent developments and insights, Dalt. Trans. 44 (2015) 448–463.
- [18] M. Zawadzka, J. Wang, W.J. Blau, M.O. Senge, Laser induced protonation of free base porphyrin in chloroform results in the enhancement of positive nonlinear absorption due to conformational distortion, J. Porphyr. Phthalocyanines 17 (2013) 1129–1133.
- [19] J. Kou, D. Dou, L. Yang, Porphyrin photosensitizers in photodynamic therapy and its applications, Oncotarget 8 (2017) 81591–81603.
- [20] P. J. Gonçalves, F.C. Bezzerra, A.V. Teles, L.B. Menezes, K.M. Alves, L. Alonso, A. Alonso, M.A. Andrade, I.E. Borissevitch, G.R. L. Souza, B.A. Iglesias, Photoinactivation of Salmonella enterica (serovar Typhimurium) by tetra-cationic porphyrins containing peripheral [Ru(bpy)2Cl]+ units, J. Photochem. Photobiol. A. 391. 112375.
- [21] D. Dolphin, The Porphyrins, Volume III, Physical Chemistry, Part A, The Porphyrins 3 (1978) 640.
- [22] M. Gouterman, Spectra of porphyrins, J. Mol. Spectrosc. 6 (1961) 138–163.
- [23] M. Gouterman, G.H. Wagnière, L.C. Snyder, Spectra of porphyrins: part II. Four orbital model, J. Mol. Spectrosc. 11 (1963) 108–127.
- [24] A. Zhang, L. Kwan, M.J. Stillman, The spectroscopic impact of interactions with the four Gouterman orbitals from peripheral decoration of porphyrins with simple electron withdrawing and donating groups, Org. Biomol. Chem. 15 (2017) 9081–9094
- [25] J.M.S. Lopes, K. Sharma, R.N. Sampaio, A.A. Batista, A.S. Ito, A.E.H. Machado, P. T. Araújo, N.M. Barbosa Neto, Novel insights on the vibronic transitions in free base meso-tetrapyridyl porphyrin, Spectrochim. Acta Part A Mol Biomol. Spectrosc. 209 (2019) 274–279.
- [26] J.M.S. Lopes, R.N. Sampaio, A.S. Ito, A.A. Batista, A.E.H. Machado, P.T. Araujo, N. M.B. Neto, Evolution of electronic and vibronic transitions in metal(II) meso-tetra (4-pyridyl)porphyrins, Spectrochim. Acta Part A Mol. Biomol. Spectrosc. 215 (2019) 327–333.
- [27] J.M.S. Lopes, R.N. Sampaio, L.R. Dinelli, A.A. Batista, P.T. Araujo, N.M.B. Neto, On the excitation dependence of fluorescence spectra of meso-tetrapyridyl zinc (II) porphyrin and its relation with hydrogen bonding and outlying decoration, Spectrochim. Acta - Part A Mol. Biomol. Spectrosc. 224 (2020), 117371.
- [28] J.M.S. Lopes, J.R.T. Reis, A.E.H. Machado, T.H.O. Leite, A.A. Batista, T.V. Acunha, B.A. Iglesias, P.T. Araujo, N.M. Barbosa Neto, Influence of the meso-substituents on the spectral features of free-base porphyrin, Spectrochim. Acta Part A Mol. Biomol. Spectrosc. 238 (2020), 118389.
- [29] J.M.S. Lopes, A.E.H. Machado, A.A. Batista, P.T. Araujo, N.M. Barbosa Neto, Protonation, exciplex, and evidence of aggregate formation in meso-tetra(4-

- pyridyl) porphyrin triggered by excited-state absorption, J. Photochem. Photobiol. A Chem. 426 (2022), 113759.
- [30] X. Chen, L. Hui, D.A. Foster, C.M. Drain, Efficient synthesis and photodynamic activity of porphyrin-saccharide conjugates: targeting and incapacitating cancer cells, Biochemistry 43 (2004) 10918–10929.
- [31] J.I.T. Costa, A.C. Tomé, M.G.P.M.S. Neves, J.A.S. Cavaleiro, 5,10,15,20-tetrakis (pentafluorophenyl)porphyrin: a versatile platform to novel porphyrinic materials, J. Porphyr. Phthalocyanines 15 (2011) 1116–1133.
- [32] J.S. Lindsey, I.C. Schreiman, H.C. Hsu, P.C. Kearney, A.M. Marguerettaz, Rothemund and adler-longo reactions revisited: synthesis of tetraphenylporphyrins under equilibrium conditions, J. Org. Chem. 52 (1987) 827–836.
- [33] P. Rothemund, Formation of porphyrins from pyrrole and aldehydes, J. Am. Chem. Soc. 57 (1935) 2010–2011.
- [34] B. Valeur, M.N. Berberan-Santos, Molecular Fluorescence: Principles and Applications, 2nd ed., Wiley-VCH Verlag & Co, Weinheim, 2012.
- [35] J.R. Lakowicz, Principles of Fluorescence Spectroscopy, 3rd ed., Springer, New York, 2006.
- [36] Y. Zhao, D.G. Truhlar, The M06 suite of density functionals for main group thermochemistry, thermochemical kinetics, noncovalent interactions, excited states, and transition elements: two new functionals and systematic testing of four M06-class functionals and 12 other function, Theor. Chem. Acc. 120 (2008) 215-241
- [37] T. Yanai, D.P. Tew, N. Chandy, A new hybrid exchange-correlation functional using the Coulomb-attenuating method (CAM-B3LYP), Chem. Phys. Lett. 393 (2004) 51–57.
- [38] A. Siiskonen, A. Priimagi, Benchmarking DFT methods with small basis sets for the calculation of halogen-bond strengths, J. Mol. Model. 23 (2017) 50.
- [39] J. Tomasi, B. Mennucci, E. Cancès, The IEF version of the PCM solvation method: An overview of a new method addressed to study molecular solutes at the QM ab initio level, J. Mol. Struct. 464 (1999) 211–226.
- [40] R.E. Skyner, J.L. McDonagh, C.R. Groom, T. van Mourik, J.B.O. Mitchell, A review of methods for the calculation of solution free energies and the modelling of systems in solution, Phys. Chem. Chem. Phys. 17 (2015) 6174–6191.
- [41] M.J. Frisch, G.W. Trucks, H.B. Schlegel, G.E. Scuseria, M.A. Robb, J.R. Cheeseman, G. Scalmani, V. Barone, B. Mennucci, G.A. Petersson, H. Nakatsuji, M. Caricato, X. Li, H.P. Hratchian, A.F. Izmaylov, J. Bloino, G. Zheng, J.L. Sonnenberg, M. Hada, M. Ehara, K. Toyota, R. Fukuda, J. Hasegawa, M. Ishida, T. Nakajima, Y. Honda, O. Kitao, H. Nakai, T. Vreven, J.A. Montgomery Jr., J.E. Peralta, F. Ogliaro, M. Bearpark, J.J. Heyd, E. Brothers, K.N. Kudin, V.N. Staroverov, T. Keith, R. Kobayashi, J. Normand, K. Raghavachari, A. Rendell, J.C. Burant, S. S. Iyengar, J. Tomasi, M. Cossi, N. Rega, J.M. Millam, M. Klene, J.E. Knox, J.B. Cross, V. Bakken, C. Adamo, J. Jaramillo, R. Gomperts, R.E. Stratmann, O. Yazyev, A.J. Austin, R. Cammi, C. Pomelli, J.W. Ochterski, R.L. Martin, K. Morokuma, V.G. Zakrzewski, G. A. Voth, P. Salvador, J.J. Dannenberg, S. Dapprich, A.D. Daniels, O. Farkas, J.B. Foresman, J.V. Ortiz, J. Cioslowski, D.J. Fox, Gaussian, Inc., Wallingford CT, 2013.
- [42] M. Presselt, W. Dehaen, W. Maes, A. Klamt, T. Martínez, W.J.D. Beenken, M. Kruk, Quantum chemical insights into the dependence of porphyrin basicity on the mesoaryl substituents: thermodynamics, buckling, reaction sites and molecular flexibility, Phys. Chem. Chem. Phys. 17 (2015) 14096–14106.
- [43] M.V. Vijisha, S. Parambath, R. Jagadeesan, C. Arunkumar, K. Chandrasekharan, Nonlinear optical absorption and optical limiting studies of fluorinated pyridyl

- porphyrins in chlorobenzene: An insight into the photo-induced protonation effects, Dye. Pigment. 169 (2019) 29–35.
- [44] W.W. Parson, Modern optical spectroscopy: With exercises and examples from biophysics and biochemistry, second edition, 2015.
- [45] C. Cohen-Tannoudji, B. Diu, F. Laloe, Quantum mechanics, Wiley, 1°., 1991.
- [46] J.M.S. Lopes, S.N. Costa, A.A. Batista, L.R. Dinelli, P.T. Araujo, N.M.B. Neto, Photophysics and visible light photodissociation of supramolecular meso-tetra(4pyridyl) porphyrin/RuCl2(CO)(PPh3)2 structures, Spectrochim. Acta - Part A Mol. Biomol. Spectrosc. 237 (2020), 118351.
- [47] E.C.A. Ojadi, H. Linschitz, M. Gouterman, R.I. Walter, J.S. Lindsey, R.W. Wagner, P.R. Droupadi, W. Wang, Sequential protonation of meso-[p-(dimethylamino) phenyl] porphyrins: charge-transfer excited states producing hyperporphyrins, J. Phys. Chem. 97 (1993) 13192–13197.
- [48] P.J. Gonçalves, L. De Boni, N.M.B. Neto, J.J. Rodrigues, S.C. Zílio, I.E. Borissevitch, Effect of protonation on the photophysical properties of meso-tetra (sulfonatophenyl) porphyrin, Chem. Phys. Lett. 407 (2005) 236–241.
- [49] A.B. Rudine, B.D. Delfatti, C.C. Wamser, Spectroscopy of protonated tetraphenylporphyrins with amino/carbomethoxy substituents: Hyperporphyrin effects and evidence for a monoprotonated porphyrin, J. Org. Chem. 78 (2013) 6040–6049.
- [50] S.E. Rodrigues, A.E.H. Machado, M. Berardi, A.S. Ito, L.M. Almeida, M.J. Santana, L.M. Liao, N.M. Barbosa Neto, P.J. Gonçalves, Investigation of protonation effects on the electronic and structural properties of halogenated sulfonated porphyrins, J. Mol. Struct. 1084 (2015) 284–293.
- [51] Y. Fang, J. Zhu, Y. Cui, L. Zeng, M.L. Naitana, Y. Chang, N. Desbois, C.P. Gros, K. M. Kadish, Protonation and electrochemical properties of pyridyl- and sulfonatophenyl-substituted porphyrins in nonaqueous media, ChemElectroChem 4 (2017) 1872–1884.
- [52] L. De Boni, C.J.P. Monteiro, C.R. Mendonça, S.C. Zílio, P.J. Gonçalves, Influence of halogen atoms and protonation on the photophysical properties of sulfonated porphyrins, Chem. Phys. Lett. 633 (2015) 146–151.
- [53] L.A. Peña, P.E. Hoggard, Photocatalysis of chloroform decomposition by hexachloroosmate(IV), Photochem. Photobiol. 86 (2010) 467–470.
- [54] R. Gilbert, M. Karabulut, P.E. Hoggard, Photocatalysis of chloroform degradation by μ-dichlorotetrachlorodipalladate(II), Inorganica Chim. Acta 363 (2010) 1462–1468.
- [55] A.J. Seidl, L.R. Cohen, L.A. Peña, P.E. Hoggard, Chlorochromate ion as a catalyst for the photodegradation of chloroform by visible light, Photochem. Photobiol. Sci. 7 (2008) 1373–1377.
- [56] L.A. Peña, A.J. Seidl, L.R. Cohen, P.E. Hoggard, Ferrocene/ferrocenium ion as a catalyst for the photodecomposition of chloroform, Transit. Met. Chem. 34 (2009) 135–141
- [57] J.A.K. Howard, V.J. Hoy, D. ÓHagan, G.T. Smith, How good is fluorine as a hydrogen bond acceptor?, Tetrahedron, 1996, 52, 12613–12622.
- [58] E. Carosati, S. Sciabola, G. Cruciani, Hydrogen bonding interactions of covalently bonded fluorine atoms: from crystallographic data to a new angular function in the GRID force field, J. Med. Chem. 47 (2004) 5114–5125.
- [59] P.A. Champagne, J. Desroches, J.-F. Paquin, Organic fluorine as a hydrogen-bond acceptor: recent examples and applications, Synthesis (Stuttg) 47 (2015) 306–322.